LA-UR-14-29009

Title: Seismic Imaging with Elastic Reverse-Time Migration

Author(s): Chen, Ting

Intended for: interview presentation

Issued: 2014-11-20

Seismic Imaging with Elastic Reverse-Time Migration

Ting Chen

Geophysics Group
Los Alamos National Laboratory
Los Alamos, NM, USA

Los Alamos NATIONAL LABORATORY EST.1943

November 21st, 2014

Introduction

- Reverse-time migration (RTM) is a powerful tool for imaging subsurface structures
  - Solves the scalar-wave equation in heterogeneous media
  - Images complex structures
- Elastic reverse-time migration (ERTM) is necessary to properly handle multicomponent seismic data
  - Solves the elastic-wave equation in heterogeneous media
  - Generates PP, SS, PS and SP images
- Some challenges in ERTM
  - low-wavenumber artifacts in PP and SS images
  - polarity reversal problem for converted-waves images (PS and SP)
  - expensive computation and memory requirement

Objective

To directly image steeply-dipping fault zones

Conventional imaging condition for ERTM

- Conventional zero-lag cross-correlation imaging condition for ERTM

$$I_{\text{xcor}}(\mathbf{x}) = \int_0^{t_{\text{max}}} S(\mathbf{x}, t) R(\mathbf{x}, t) dt$$

I_{xcor}: image

t_{max}: the maximum record time

$S(\mathbf{x}, t)$: forward-propagated source wavefield

$R(\mathbf{x}, t)$: backward-propagated receiver wavefield

$S(\mathbf{x}, t)$ and $R(\mathbf{x}, t)$ can be either P or S component

Images: I_{PP}, I_{PS}, I_{SP}, I_{SS}

Conventional imaging condition for ERTM

- Pro
  - straightforward
  - easy to implement
- Con
  - generates low-wavenumber migration artifacts
    - for I_{PP} and I_{SS}
    - particularly strong for high-contrast, sharp interfaces
    - may mask some crucial structures
  - produces destructive images due to polarity reversal
    - for I_{PS} and I_{SP}
  - is difficult to obtain clear images of steeply-dipping fault zones

Imaging condition with wavefield separation

- Separate the forward and backward propagation wavefields into downgoing, upgoing, leftgoing, and rightgoing wavefields
- Obtain downward-looking (I^d), upward-looking (I^u), left-looking (I^l), and right-looking (I^r) images

$$
\begin{aligned}
I^d(\mathbf{x}) &= \int_0^{t_{\max}} S^{+z}(\mathbf{x},t)R^{-z}(\mathbf{x},t)dt \\
I^u(\mathbf{x}) &= \int_0^{t_{\max}} S^{-z}(\mathbf{x},t)R^{+z}(\mathbf{x},t)dt \\
I^l(\mathbf{x}) &= \int_0^{t_{\max}} S^{-x}(\mathbf{x},t)R^{+x}(\mathbf{x},t)dt \\
I^r(\mathbf{x}) &= \int_0^{t_{\max}} S^{+x}(\mathbf{x},t)R^{-x}(\mathbf{x},t)dt
\end{aligned}
$$

- $I = I^d + I^l + I^r$

Polarity correction for converted waves

- The Poynting vector **F** describes the energy flux density

$$\mathbf{F} = -\dot{p}\,\nabla p$$

p: the wavefield quantity for P or S waves

- can be used to correct for polarity reversal

$$I(\mathbf{x}) = \int_0^{t_{\max}} S(\mathbf{x}, t) R(\mathbf{x}, t) sgn(\mathbf{F}_s \times \mathbf{F}_r) dt$$

- computationally efficient
- difficult to obtain accurate estimate for complicated wavefields

Polarity correction for converted waves

- combine the Poynting-vector method with wavefield separation

$$I^d(\mathbf{x}) = \int_0^{t_{\max}} S^{+z}(\mathbf{x},t)R^{-z}(\mathbf{x},t)sgn(\mathbf{F}_s^{+z} \times \mathbf{F}_r^{-z})dt,$$

$$I^u(\mathbf{x}) = \int_0^{t_{\max}} S^{-z}(\mathbf{x},t)R^{+z}(\mathbf{x},t)sgn(\mathbf{F}_s^{-z} \times \mathbf{F}_r^{+z})dt,$$

$$I^l(\mathbf{x}) = \int_0^{t_{\max}} S^{-x}(\mathbf{x},t)R^{+x}(\mathbf{x},t)sgn(\mathbf{F}_s^{-x} \times \mathbf{F}_r^{+x})dt,$$

$$I^r(\mathbf{x}) = \int_0^{t_{\max}} S^{+x}(\mathbf{x},t)R^{-x}(\mathbf{x},t)sgn(\mathbf{F}_s^{+x} \times \mathbf{F}_r^{-x})dt,$$

- more accurate estimate of Poynting vectors
- better image the steeply-dipping fault zones

90-deg fault model

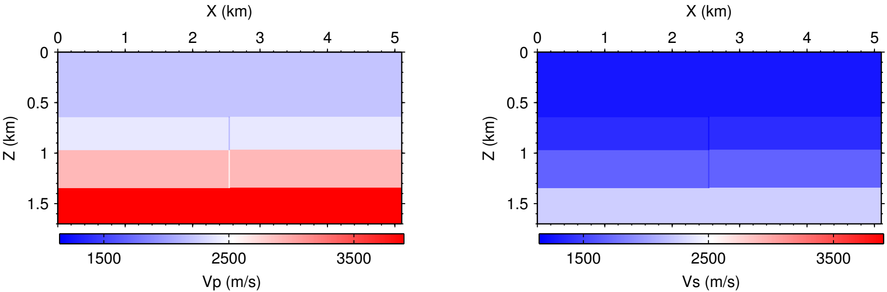

P-wave velocity

S-wave velocity

- fault zone thickness: 20 m
- fault zone velocity: 10% lower than surrounding regions
- $V_P / V_S = 1.73$

PP images

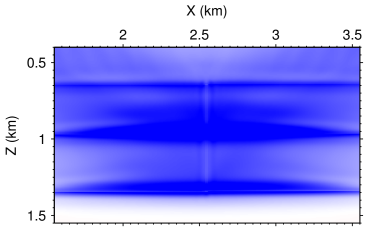

Conventional ERTM

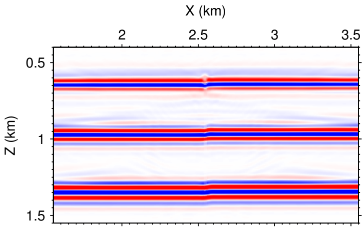

Downward looking

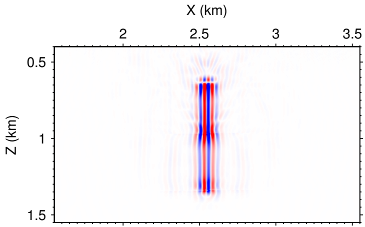

Horizontal looking

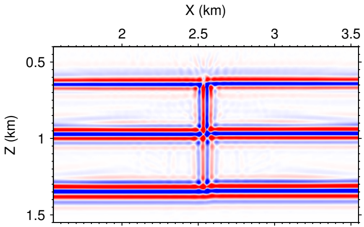

Our ERTM

PS images

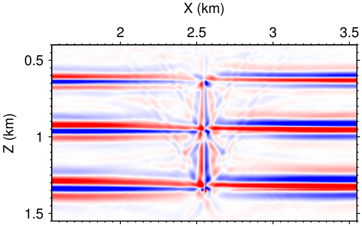

Conventional ERTM

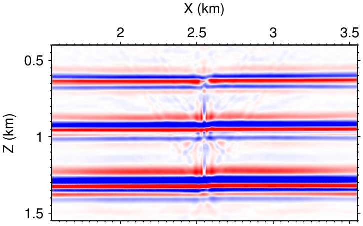

With polarity correction

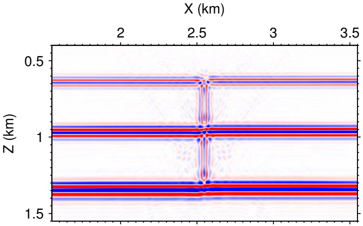

Our ERTM

Soda Lake velocity model

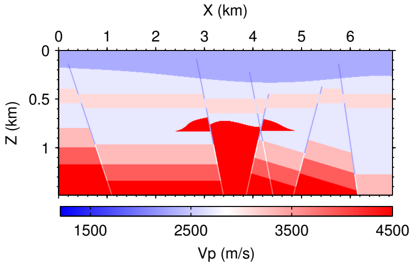

P-wave velocity

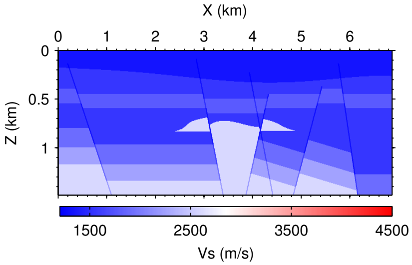

S-wave velocity

- Soda Lake geothermal field, Nevada
- based on geologic interpretation result of a prestack migration image
- fault zone thickness: 25 m
- fault zone velocity: 15% lower than surrounding regions
- $V_P / V_S = 1.73$

PP images

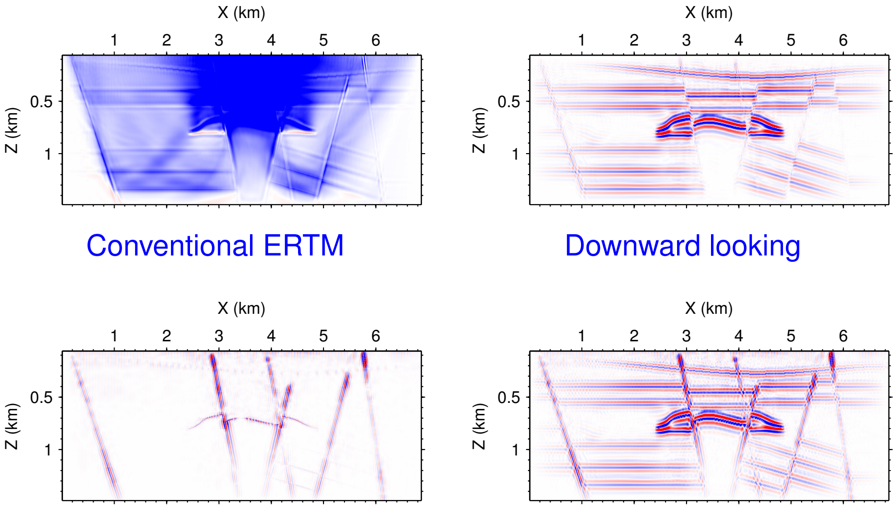

Conventional ERTM

Downward looking

Horizontal looking

Our ERTM

PS images

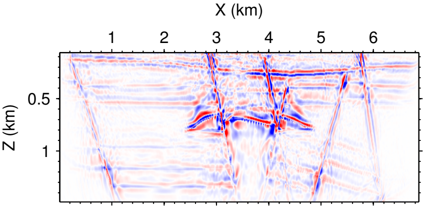

Conventional ERTM

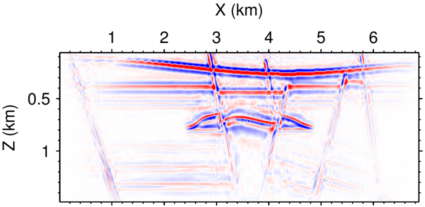

With polarity correction

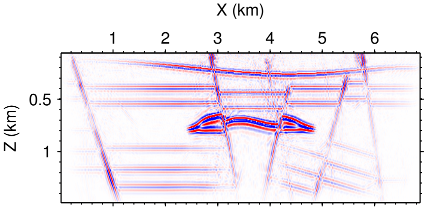

Our ERTM

Conclusions

- We have developed a new imaging condition for ERTM by combing the Poynting-vector method and wavefield separation in both vertical and horizontal directions
- Our new imaging condition can directly image steeply-dipping fault zones
- Our new imaging condition can eliminate low-wavenumber artifacts
- Our new imaging condition can efficiently correct polarity reversals
- We have demonstrated using synthetic examples that our new imaging condition greatly improves the images of steeply-dipping fault zones

Objective

To develop a new imaging condition for ERTM

- Eliminate low-wavenumber image artifacts
- Reduce the computational cost and the computer memory requirement of implementing the imaging condition

Concepts

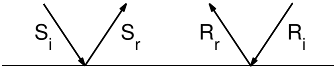

S: source wavefield

R: receiver wavefield

i: incident

r: reflected

$$
\begin{aligned}
I_{\text{xcor}} &= \int S \cdot R \cdot dt \\
&= \int (S_i + S_r) \cdot (R_i + R_r) \cdot dt \\
&= \int S_i \cdot R_i \cdot dt + \int S_r \cdot R_r \cdot dt \\
&\quad + \int S_r \cdot R_i \cdot dt + \int S_i \cdot R_r \cdot dt
\end{aligned}
$$

Amplitude

$$S_i > S_r$$

$$R_i > R_r$$

Excitation amplitude imaging condition

- During the forward propagation of the source wavefield, for each imaging point, we store
  - the maximum amplitude of the wavefield (S_i)
  - its corresponding excitation time t_0

- Rather than using

$$I_{\text{xcor}}(\mathbf{x}) = \int_0^{t_{\max}} S(\mathbf{x}, t) R(\mathbf{x}, t) dt,$$

  we can simply use

$$I(\mathbf{x}) = S(\mathbf{x}, t_0(\mathbf{x})) \cdot R(\mathbf{x}, t_0(\mathbf{x}))$$

$$\Longrightarrow \quad S_i \cdot (R_i + R_r) \qquad \sout{S_r \cdot (R_i + R_r)}$$

Excitation amplitude imaging condition

- To further remove artifacts $S_i \cdot (R_i + \cancel{R_r})$
- Determine the excitation time $t_{0\mathrm{R}}$ for receiver wavefield

$t_{0\mathrm{R}}$: corresponding to the maximum amplitude of wavefield within $[t_0 - T \quad t_f]$
T: $\approx$ a half period for the central frequency
t_f: model dependent

  - velocities gradually increase with depth: $t_f = t_{\max}$
  - there is a sudden large velocity jump : $t_f(\mathbf{x}) = t_0(\mathbf{x}) + f(d(\mathbf{x}), V(\mathbf{x}))$
    d: layer thickness
    we use $f \approx 1.5d(\mathbf{x})/V(\mathbf{x})$

New imaging condition

$$I(\mathbf{x}) = \begin{cases} 0 & \text{if } |t_0(\mathbf{x}) - t_{0R}(\mathbf{x})| > T \\ S(\mathbf{x}, t_0(\mathbf{x})) \cdot R(\mathbf{x}, t_0(\mathbf{x})) & \text{if } |t_0(\mathbf{x}) - t_{0R}(\mathbf{x})| \le T \end{cases}$$

PP images for a two-layer model

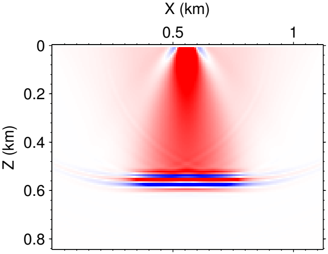

Conventional imaging

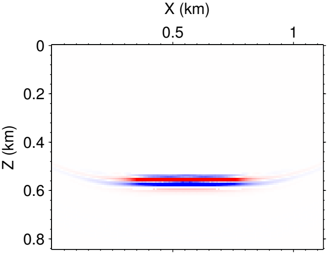

New excitation amplitude imaging

PP images for a multiple-layer model

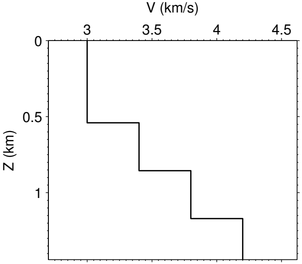

Velocity model

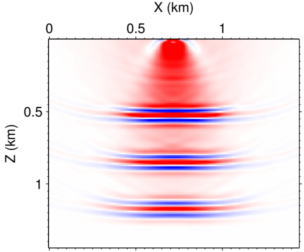

Conventional imaging

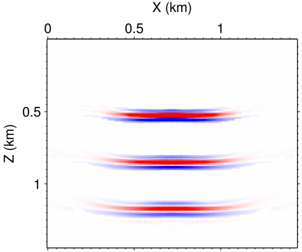

New excitation amplitude imaging

PP images for a model with sudden V jump

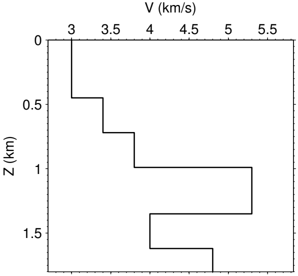

Velocity model

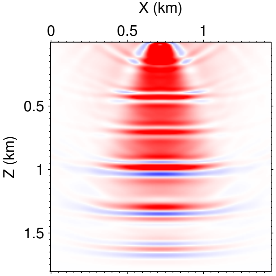

Conventional imaging

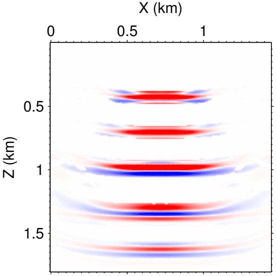

New excitation amplitude imaging

PS images for a model with sudden V jump

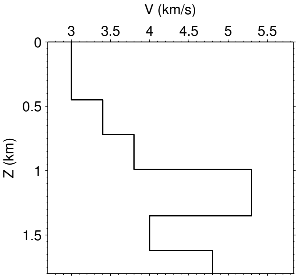

Velocity model

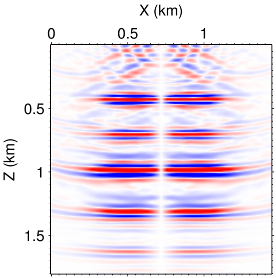

Conventional imaging

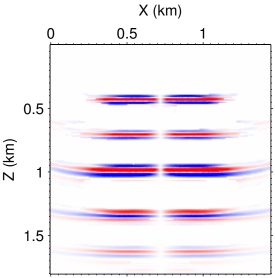

New excitation amplitude imaging

Conclusions

- We have developed a new excitation amplitude imaging condition for ERTM
- Our new imaging condition can eliminate migration artifacts
- Our new imaging condition can also reduce the computational cost and the computer-memory requirement
- We have demonstrated the effectiveness of our new imaging condition using synthetic data for layered models
  - PP
  - PS
- Future work: test on more complex models

Acknowledgements

- This work was supported by the U.S. Department of Energy through contract DE-AC52-06NA25396 to Los Alamos National Laboratory.
- The computation was performed on super-computers provided by the Institutional Computing Program of Los Alamos National Laboratory.